# Structural properties of effective potential model by liquid state theories

Xiang Yuan-Tao(向远涛)[a], Andrej Jamnik[b], and Yang Kai-Wei(杨开巍)[a]†

[a] School of Physics Science and Technology, Central South University, Changsha 410083, China
[b] University of Ljubljana, Faculty of Chemistry and Chemical Technology, Aškerčeva 5, SI-1001 Ljubljana, Slovenia

(Received 30 April 2009; revised manuscript received 29 May 2010)

This paper investigates the structural properties of a model fluid dictated by an effective inter-particle oscillatory potential by grand canonical ensemble Monte Carlo (GCEMC) simulation and classical liquid state theories. The chosen oscillatory potential incorporates basic interaction terms used in modeling of various complex fluids which is composed of mesoscopic particles dispersed in a solvent bath, the studied structural properties include radial distribution function in bulk and inhomogeneous density distribution profile due to influence of several external fields. The GCEMC results are employed to test the validity of two recently proposed theoretical approaches in the field of atomic fluids. One is an Ornstein–Zernike integral equation theory approach; the other is a third order + second order perturbation density functional theory. Satisfactory agreement between the GCEMC simulation and the pure theories fully indicates the ready adaptability of the atomic fluid theories to effective model potentials in complex fluids, and classifies the proposed theoretical approaches as convenient tools for the investigation of complex fluids under the single component macro-fluid approximation.

**Keywords:** atomic fluid, classical ensemble

**PACC:** 0520G

## 1. Introduction

Atomic fluid classical density functional theory (DFT) was extensively investigated and applied during the last three decades, and has evolved into a powerful tool for classical liquid state matters. To be specific, the classical DFT approach plays indispensable roles in various fields such as calculation of density profiles,[1] supercritical adsorption,[2] cavity formation energy,[3−5] solvation forces,[6] interface behaviours[7] and so on.[8−10] In the classical DFT, a crucial entity is the free energy density functional $F[\rho]$ for an inhomogeneous system with $\rho(\boldsymbol{r})$ a single particle density distribution. As $F$ is a summary between ideal part $F_{\rm id}$ and excess part $F_{\rm ex}$ and the $F_{\rm id}$ is exactly known, then what has to be approximated is the excess part $F_{\rm ex}$. Hence main effort in developing the classical DFT is devoted to approximating $F_{\rm ex}$ or a non-uniform first order direct correlation function (DCF) $C^{(1)}(\boldsymbol{r},[\rho])$, namely, the first order functional derivative of $-\beta F_{\rm ex}[\rho]$ w.r.t. $\rho(\boldsymbol{r})$. Throughout the present paper, $\beta = 1/kT$ with $k$ a Boltzmann's constant and $T$ an absolute temperature. Upon acquirement of $C^{(1)}(\boldsymbol{r},[\rho])$, one can obtain $F_{\rm ex}$ by means of a functional integration method as shown in Refs. [11]–[13]. As a general rule, one employs the atomic fluid as an initial test sample to examine the reliability of any density functional approximation (DFA) proposed. The atomic fluid is in general characterised by a model potential comprised of a highly steep repulsion at closest separation and a monotonously weakening attraction at far inter-particle separation. However a feature specific to effective potentials dominating over phase behaviours of complex fluids is a vibrating decay of the potential as a function of the separation between two particles. Although perturbation part of the potential only supplies small correction to hard sphere equation of state and structural functions, main features of a general van der Waals fluid stem from the perturbation part. As the perturbation part of the effective potential apparently differs from that of the atomic model potential, there is a necessity to examine whether any DFA suiting the atomic model fluid is also fit for the effective model potential.

Before we start the examination, it is possible to give a brief historical retrospect about the development of classical DFT. Particular attention will be given to Zhou's contribution[11−13] to the classical

†Corresponding author. E-mail: kwyang@issp.ac.cn

© 2010 Chinese Physical Society and IOP Publishing Ltd

DFT as the chosen third order + second order perturbation DFT approach is due to this author. The first application of the classical DFT was reported by Ebner *et al.*,[14] in an excellent review paper[15] Evans gave a self-contained account of the classical DFT formalism. A highly developed domain of the classical DFT is in the inhomogeneous hard sphere fluid for which several reliable DFAs are available. To list some of them, we have a well-known weighted density approximation (WDA) respectively due to Nordholm and co-workers,[16,17] Tarazona,[18] Curtin and Ashcroft;[19] a variant of the WDA, namely, the fundamental measure functional due to Rosenfeld,[20] Kierlik and Rosinberg and others.[21−23] A traditional functional perturbation expansion approximation was also developed greatly by Zhou and coworkers through truncating the expansion at higher order[24] and through including all of the terms in the form of a second order truncation.[25−29] Finally, the most simple and accurate hard sphere DFA is a so-called bridge density functional approximation due to Zhou and co-workers[30,31] and Zhou.[32−36] Straightforward extension of the hard sphere WDA to van der Waals fluid is frustrated by the existence of the non-stable region in the phase diagram. Zhou also proposes a methodology[37,38] for formulating DFA by integrating the information of bulk fluid radial distribution function (RDF), the resulted DFA is in principle adaptable to extension to the van der Waals fluid, but much work still needs to be done.

The theoretical progress aimed for non-hard sphere fluids falls behind greatly. Until several years ago, the most generally used approximation is still a crude van der Waals mean field approximation for tail contribution.[39] Only in recent years, several new non-hard sphere DFAs are proposed by different authors. One is a hard sphere WDA plus tail WDA[40−44] in which the hard core part and tail term are separately treated by different WDAs, the other is a so-called third order + second order perturbation DFT[45,46] whose adaptability to effective model potential will be examined in the present work. Finally, a universal theoretical way is proposed by Zhou[47−53] which is readily adaptable to any non-hard sphere fluids; it has been confirmed that the universal theoretical way[47−53] actually leads to the most accurate DFT formalism for non-hard sphere fluids studied. As for the application of the classical DFT approach, there is much to be said. By considering the solid phase as a highly inhomogeneous liquid phase, the classical DFT approach finds wide applications in solid-liquid phase transition;[54] electrical double layer phenomena have also been investigated in detail by the classical DFT approach;[55−57] in combination with an Ornstein–Zernike (OZ) integral equation theory the classical DFT approach plays key role in calculation of potential of mean force.[58−65] Finally the classical DFT approach greatly pushes the investigation of the polymer chain molecules near surfaces.[66−71]

The aim of the present paper is to apply a recent third order + second order perturbation DFT to an effective potential model and examine the adaptability of the chosen approach to the chosen effective model potential. The organisation of the paper is as follows. In Section 2 we will recapitulate the essentials and numerical particulars of the third order + second order perturbation DFT, and describe thoroughly the chosen effective model potential. The simulation method will also be briefly outlined in this section. In Section 3 the theoretical calculation results and simulation results are presented and compared with each other, structural features particular to the effective potential fluid are described. Finally our conclusions are drawn in Section 4.

## 2. Methods and models

### 2.1. Model

In the present work the interactions between the particles are represented by a shifted effective potential with energy parameter $\varepsilon$, hard core diameter $\sigma$:

$$u_{\rm ts}(r)=\begin{cases}\propto, & r<\sigma,\\ u(r)-u(r_{\rm c}), & \sigma\le r<r_{\rm c},\\ 0, & r\ge r_{\rm c}\end{cases} \tag{1}$$

with

$$u(r)/\varepsilon=\begin{cases}\propto, & r<\sigma,\\ (\varepsilon_{\rm b}+1)(r/\sigma-1)/(b-1)-1, & \sigma\le r\le b,\\ \varepsilon_{\rm b}\exp\left(-\alpha\left(\frac{r}{\sigma}-b\right)\right)\cos\left[k_{\rm s}\left(\frac{r}{\sigma}-b\right)\right]\Big/\left(\frac{r}{b\sigma}\right)^{n}, & r>b,\end{cases} \tag{2}$$

where $r_c$ is the distance at which the potential is truncated and shifted, and $b$, $\alpha$, $k_s$, $n$, and $\varepsilon_b$ are parameters defining the precise form of the potential, and are connected with the solvent bath properties by means of very complicated relationships, the explicit mathematical form is beyond the scope of the present paper. The part with $b \geq r/\sigma \geq 1$ reflects the depletion attraction[72,73] induced by the finite size of the solvent particles and the part for $b < r/\sigma$ reflects the packing effect of the solvent particles. By properly choosing the parameters, the potential Eqs. (1) and (2) not only mimics the shape of the potential arising in depletion interactions, but also other kinds of interactions, such as the effective interionic pair potentials in some alkali metals[74] and alloys.[75] Bulk thermodynamic properties of fluid dictated by the potential function Eqs. (1) and (2) are investigated in Ref. [76] by canonical (NVT) ensemble Monte Carlo (MC) simulations and a recent third order thermodynamic perturbation theory.[77−81]

We will investigate two kinds of structure function, one is represented by a RDF suitable for description of bulk fluid, the other is denoted by density distribution function $\rho(\boldsymbol{r})$ suitable for characterisation of the fluid subjected to various external fields.

The external fields of interest are comprised of different spatial constraints. Besides the single hard wall, we treat also a spherical cavity surrounded by the spherical hard wall, a planar gap, i.e. the two hard walls separated by a distance $L$, and a hard spherical particle, the corresponding external potentials $\phi_{\text{ext}}$ are

$$\phi_{\text{ext}}(z) = \begin{cases} 0, & z > \dfrac{1}{2}\sigma, \\ \infty, & \text{otherwise} \end{cases} \tag{3}$$

for a single hard wall,

$$\phi_{\text{ext}}(r) = \begin{cases} 0, & r < R - \dfrac{1}{2}\sigma, \\ \infty, & \text{otherwise} \end{cases} \tag{4}$$

for a spherical cavity with hard spherical wall of radius $R$,

$$\phi_{\text{ext}}(z) = \begin{cases} 0, & \dfrac{1}{2}\sigma < z < L - \dfrac{1}{2}\sigma, \\ \infty, & \text{otherwise} \end{cases} \tag{5}$$

for a planar slit with two plane hard walls situated at $z = 0$ and $z = L$, respectively, and

$$\phi_{\text{ext}}(r) = \begin{cases} 0, & r > \dfrac{1}{2}(R + \sigma), \\ \infty, & \text{otherwise} \end{cases} \tag{6}$$

for a hard spherical particle of diameter $R$.

## 2.2. Third order + second order perturbation DFT

In the third order + second order perturbation DFT approach[46,82,83] the hard core part (denoted by subscript hc) of the interaction potential is treated by the third order functional perturbation expansion approximation (FPEA),[24] while the tail part (denoted by subscript tail), whose dependence on the density argument is very weak, is proved to be treated sufficiently by the second order FPEA.[45] The third order + second order perturbation DFT approach is shown to be very reliable for diverse inhomogeneous fluids[82,83] on condition that the input information, i.e. the bulk second order direct correlation function (DCF) $C_0^{(2)}(\boldsymbol{r}; \rho_b \ldots)$, is sufficiently reliable. In classical DFT, the $\rho(\boldsymbol{r})$ conforms to a density profile equation

$$\rho(\boldsymbol{r}) = \rho_b \exp\left\{-\beta\varphi_{\text{ext}}(\boldsymbol{r}) + C^{(1)}(\boldsymbol{r}; [\rho]\ldots) - C_0^{(1)}(\rho_b \ldots)\right\}, \tag{7}$$

here, $\varphi_{\text{ext}}(\boldsymbol{r})$ is an external potential responsible for formation of the inhomogeneous spatial density profile $\rho(\boldsymbol{r})$, $\rho_b$ is density of the coexistence bulk with which the inhomogeneous system under consideration is in equilibrium, $C^{(1)}(\boldsymbol{r}; [\rho]\ldots)$ and $C_0^{(1)}(\rho_b \ldots)$ are respectively inhomogeneous and homogeneous first order DCF of the system of interest. Difference of $C^{(1)}(\boldsymbol{r}; [\rho]\ldots)$ and $C_0^{(1)}(\rho_b \ldots)$ is given in the third order +second order perturbation DFT approach by

$$\begin{aligned} & C^{(1)}(\boldsymbol{r}; [\rho]\ldots) - C_0^{(1)}(\rho_b \ldots) \\ = & \int \mathrm{d}\boldsymbol{r}' \left[\rho(\boldsymbol{r}') - \rho_b\right] C_0^{(2)}(|\boldsymbol{r} - \boldsymbol{r}'|; \rho_b \ldots) + \frac{C_{0hc}^{(1)''}(\rho_b \ldots)}{2\left[C_{0hc}^{(1)'}(\rho_b \ldots)\right]^3} \int C_{0hc}^{(2)}(\boldsymbol{r}, \boldsymbol{r}''; \rho_b \ldots) \\ & \times \left[\int C_{0hc}^{(2)}(\boldsymbol{r}', \boldsymbol{r}''; \rho_b \ldots)\left(\rho(\boldsymbol{r}') - \rho_b\right) \mathrm{d}\boldsymbol{r}'\right]^2 \mathrm{d}\boldsymbol{r}''. \end{aligned} \tag{8}$$

Ordinarily the coefficient $C_{0\mathrm{hc}}^{(1)}(\rho_\mathrm{b}\ldots)/2[C_{0\mathrm{hc}}^{(1)'}(\rho_\mathrm{b}\ldots)]^3$ is substituted by an adjustable parameter $\lambda$ determined by a single hard wall sum rule[84] which claims knowledge of pressure of the coexistence bulk fluid. Because of possible small errors associated with the bulk pressure calculated by any theoretical route, which can then interfere the reliability of the judgment on the quality of the performance of the DFT approach, we utilise the simulation result for the pressure as an input, its value is equal to $\rho\,(0.5\sigma)/\beta$. This means that the parameter $\lambda$ is adjusted to a value ensuring an equality of the single hard wall contact density predicted by the present DFT approach and that obtained by 'exact' simulation method. Nevertheless, in practical cases one could also use the pressure based on the OZ integral equation theory. Although this would give rise to small quantitative errors in the calculations, it would not affect the qualitative features of the final results.

The $C_{0\mathrm{hc}}^{(2)}(r;\rho_\mathrm{b}\ldots)$, a hard core part of $C_0^{(2)}(r;\rho_\mathrm{b}\ldots)$, is obtained by disposing of the tail part $C_{0\mathrm{tail}}^{(2)}(r;\rho_\mathrm{b}\ldots)$ from the $C_0^{(2)}(r;\rho_\mathrm{b}\ldots)$, i.e. one has

$$\begin{aligned} &C_0^{(2)}(r;\rho_\mathrm{b}\ldots)\\ &=C_{0\mathrm{hc}}^{(2)}(r;\rho_\mathrm{b}\ldots)+C_{0\mathrm{tail}}^{(2)}(r;\rho_\mathrm{b}\ldots). \end{aligned} \tag{9}$$

As a matter of course, $C_{0\mathrm{hc}}^{(2)}(r;\rho_\mathrm{b}\ldots)$ corresponds to highly steep repulsion core, thus one has

$$C_{0\mathrm{hc}}^{(2)}(r;\rho_\mathrm{b}\ldots)=\begin{cases} C_0^{(2)}(r;\rho_\mathrm{b}\ldots), & r<r_\mathrm{cut}\\ 0, & r>r_\mathrm{cut}, \end{cases} \tag{10}$$

and

$$C_{0\mathrm{tail}}^{(2)}(r;\rho_\mathrm{b}\ldots)=\begin{cases} 0, & r<r_\mathrm{cut},\\ C_0^{(2)}(r;\rho_\mathrm{b}\ldots), & r>r_\mathrm{cut}. \end{cases} \tag{11}$$

Here $r_\mathrm{cut}$ is the cutting distance at which the bulk second order DCF is split into the hard-core part and tail part. For the potential of present interest, the hard sphere diameter $\sigma$ should obviously be chosen as the value for $r_\mathrm{cut}$.

Attainability of the $C_0^{(2)}(r;\rho_\mathrm{b}\ldots)$ is obtained by way of the OZ integral equation theory which is summarized as follows.

## 2.3. The OZ integral equation theory

The OZ integral equation theory supplies not only the RDF describing the bulk structural properties but also the bulk second order DCF as input of the classical DFT approach. The OZ integral equation theory is characterised by a well-known OZ integral equation given by Eq. (12) supplemented by a close equation given by Eq. (13).

$$\begin{aligned} h(r)=&C_0^{(2)}(r;\rho_\mathrm{b}\ldots)+\rho_\mathrm{b}\int \mathrm{d}\boldsymbol{r}_1\,h\\ &\times(\boldsymbol{r}_1)\,C_0^{(2)}(|\boldsymbol{r}-\boldsymbol{r}_1|;\rho_\mathrm{b}\ldots). \end{aligned} \tag{12}$$

$$h(r)+1=\exp\{-\beta u(r)+\gamma+B(r)\}, \tag{13}$$

here $h(r)=g(r)-1$ is a total correlation function, and $\gamma(r)=h(r)-C_0^{(2)}(r;\rho_\mathrm{b}\ldots)$ is an indirect correlation function at the specified values of the model parameters, the bulk density $\rho_\mathrm{b}$ and others. The $B(r)$ is a so-called bridge function, which is a sum of 'bridge' or 'elementary' graphs in the diagrammatic analysis of the two-point functions.[85] A recently proposed bridge function approximation[86] for a Lennard–Jones (LJ) fluid will be applied to the present model effective potential, and its numerical particulars are recapitulated as follows. Reference [86] proposed a so-called GvEF-BS-VW hard sphere bridge function

$$B_\mathrm{hs}(r)=\begin{cases} \ln(y_\mathrm{hs}(r))+1+C_{0\mathrm{hs}}^{(2)}, & (r)\,r<\sigma_\mathrm{hs},\\ \ln(g_\mathrm{hs}(r))+C_{0\mathrm{hs}}^{(2)}(r)+1-g_\mathrm{hs}(r), & r>\sigma_\mathrm{hs}, \end{cases} \tag{14}$$

here $y_\mathrm{hs}(r)$, $C_{0\mathrm{hs}}^{(2)}(r)$ and $g_\mathrm{hs}(r)$ are respectively cavity correlation function, bulk second order DCF and RDF of the hard sphere fluid with a diameter $\sigma_\mathrm{hs}$. It has been shown that a combination of the GvEF–BS–VW hard sphere bridge function and the modified hypernetted chain approximation[87] for the closure of the OZ integral equation performs very well for the Lennard–Jones fluid.[86]

The MHNC approximation is associated with an adjustable parameter, i.e. an effective hard sphere diameter $d^*$ whose value is specified by a local thermodynamic self-consistency condition. For the details about the numerical procedure, we refer the readers to Ref. [86]. Upon numerical solution of the OZ integral equation, one obtains the RDF $g(r)$, which is compared with the corresponding simulation data, and the

bulk second DCF $C_0^{(2)}(r;\rho_{\rm b}\ldots)$, which is used as an input for the third order + second order perturbation DFT.

## 2.4. Open ensemble simulation

The MC simulations were performed within the grand canonical ensemble by using the Metropolis[88] simulation technique. In the open ensemble, the chemical potential $\mu$, the volume $V$, and the temperature $T$ of the system are fixed, while the number of particles $N$ is allowed to fluctuate. This set of independent parameters defined by the thermodynamic state of the system makes possible the study of the equilibrium between the fluid in the homogeneous phase and the same fluid being subjected to some external field, which causes the spatial inhomogeneity in the structure of the fluid. This inhomogeneous structure we first determined for the simplest and quite usual geometry is considered in theoretical studies of confined fluids, that is a planar slit consisting of two parallel, perfectly smooth hard walls at a specified separation $L$. The actual distance accessible for the fluid was therefore $L$–$\sigma$. Denote the perpendicular direction by $z$, then the fluid between the walls extended to infinity along the directions $x$ and $y$, flows parallel to the walls. In practical simulations, the system was modeled as an infinite array of identical simulation cells of the volume $L \times a^2$, repeating themselves in the two lateral directions, along which the minimum image convention was applied. No periodicity needed to be assumed in the direction $z$ normal to the plates. In addition, when modeling wide enough pores, where there exist domains of the fluid sufficiently distant from both walls to retain practically nonperturbed density and other properties of the bulk phase, it could be accepted that the structure of the fluid at either plate did not appear to be affected by the presence of the opposite wall. These results should therefore be almost identical to the density profiles next to isolated walls or walls at infinite separations. This way, the structure of the fluid near a hard, flat interface was considered. In most cases, the value for the width of the gap $L = 20\sigma$ was sufficient to avoid the interference between the symmetrical density profiles at individual walls of the pore. Further external field considered by us was imposed by the presence of the closed spherical surface mimicking a spherical cavity of the radius $R$. In this case, as the MC cell was a closed pool of the fluid, there was no need for using the periodic boundary conditions. Finally, we turned some attention to the structure of the fluid near a single hard sphere. For this system, similarly as in the case of simulation of homogeneous (bulk) phase, the MC cell was a cubic box of the volume $a^3$ with the periodic boundary conditions imposed in all three directions. The fluid surrounded a hard sphere located at the centre of the cell.

During the simulation, the phase space was sampled through alternating canonical MC (CMC) and grand canonical MC (GCMC) steps, i.e. by the movement of randomly chosen particle, and by the addition to or removal of particles from the system. Additions and removals were attempted randomly with a probability $P$, so the probability for the move of a randomly chosen particle was $1-2P$. The value $P \approx 0.15$ was used in most of our runs. A new configuration was first checked for a hard-core overlap. It was automatically rejected if the overlap had been detected. In restricted geometry, the rejection applied to the moves or additions leading to an overlap of the moved or added particle with another molecule or with the boundaries of the confinement. After this check, the moves were accepted with the probability $f_{ij}$ given by

$$f_{ij} = \min\{1, \exp[-\beta(u_j - u_i)]\}, \qquad (15)$$

where $\beta$ has its usual meaning, $\beta = 1/kT$. The subscripts $i$ and $j$ denote the initial and the attempted configuration respectively; $u_j - u_i$ is the change of the total configurational potential energy due to the particle move. Additions and removals were accepted with the probabilities[88]

$$\begin{cases} f_{ij} = \min\{1, r\}, & \text{for addition,} \\ f_{ji} = \min\{1, 1/r\}, & \text{for removal,} \end{cases} \qquad (16)$$

where

$$r = \frac{\rho_{\rm b}}{\rho_{\rm j}} \exp[\beta(\mu_{\rm b}^{\rm ex} - u_j + u_i)]. \qquad (17)$$

Above, the subscript $ij$ denotes an increase and $ji$ a decrease in the number of particles, i.e., $N_j = N_i + 1$. The $\rho_{\rm b}$ and $\mu_{\rm b}^{\rm ex}$ are the mean number density and excess chemical potential of the bulk phase respectively, $u_j - u_i$ is the energy change due to the addition or deletion of a particle. The values for the excess chemical potential $\mu_{\rm b}^{\rm ex}$ for the prescribed (targeted) bulk densities were determined by using iterative GCMC algorithm.[89]

The density profiles were determined from the average numbers of the particles found within the slices

into which the elementary MC cell was subdivided. A typical duration of a GCMC run was about $2 \times 10^6$ trial moves per particle in the production calculation, and $5 \times 10^5$ moves per particle were needed to equilibrate the system. The allowed displacement of the moved particle was usually restricted to ascertain a move acceptance of about 60%.

We have not estimated errors in simulations, but the results are of high accuracy because we performed very long runs (about $2.5 \times 10^9$ configurations) to achieve good statistics. Hence, the error bars are very small, and the simulation results can serve as a fair comparison.

## 3. Results and discussion

In the following we present the theoretical and simulation results for the homogeneous and inhomogeneous structures of the fluid with underlying interaction potential given by Eqs. (1) and (2). We perform calculations for one set of potential parameters: $b = 1.15,\ \alpha = 1.0,\ k_{\rm s} = 12,\ n = 3,\ \varepsilon_{\rm b} = 0.5$. The investigation is performed at supercritical situations by fixing the reduced temperature $T^* = kT/\varepsilon$ of the coexisting bulk fluid at the highest values simulated in Ref. [76], i.e. $T^* = 1.1$.

In Fig. 1 we present the RDF of the bulk fluid for the chosen set of potential parameters and at different densities, whereas Figs. 2–5 show the density profiles of the same fluid: (i) at a single hard wall (Fig. 2); (ii) in the planar gap of width $L = 4\sigma$ (Fig. 3); (iii) in the spherical cavity of radius $R = 4\sigma$ (Fig. 4); (iv) near a hard spherical particle of radius $R = 0.7\sigma$ (Fig. 5). For the sake of clarity, the majority of these figures are subdivided into three parts, which successively illustrate the effect of increase in the bulk density at constant values of potential parameters.

The theoretical RDFs shown in Fig. 1 are computed by solving the OZ integral equation along with the bridge function approximation.[86] As in narrow domain close to contact distances the underlying potential is attractive, this gives rise to high contact values of $g(r)$ and deep minima at the distances slightly exceeding the contact values. These minima stem from the exclusion volume effect of the molecular layer firmly attached to the central particle, and, in addition, from the fact that the linear attractive part in the potential function at $r < b\sigma$ is followed by the repulsive part of the first oscillating cycle. At higher distances the shape of $g(r)$ is oscillatory due to the layering structure of the fluid. It is interesting to observe that the period of oscillations approximately coincides with that in the potential function, i.e., the minima in $g(r)$ approximately coincide with the maxima (repulsion) in the oscillatory potential function and vice versa. Rapid look at the computed RDFs indicates excellent agreement between the results obtained by the approximate integral equation theory and simulation data.

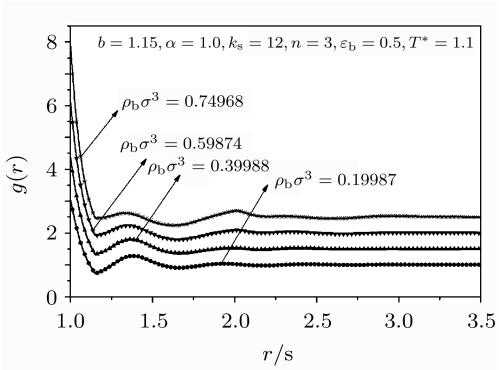



**Fig. 1.** The DFT (lines) and simulation (symbols) results for the RDF of the bulk fluid for one set of potential parameters as described in the figure and at different densities.

The results for the inhomogeneous structure of the fluid subjected to diverse external fields are displayed in Figs. 2–5 which show the structural features peculiar to the behaviour of the fluids at the interfaces and in confined systems. A general course of the density profiles is that a flat density profiles $\rho(x) = \rho_{\rm b}$ are restored at sufficient distances from the wall, irrespective of the specific nature of the intermolecular potential and the external field parameters. Upon approaching the wall these interactions begin to compete with steric effects. This competition, of course, is now strongly dependent on the particular intermolecular potential and in addition, on the temperature of the system. In any case, the inter-particle interactions have a stronger influence on the structure of the fluid at lower temperatures. As the strongly attractive molecules have a better chance for mutual attraction at sufficient distances from the wall(s) or outside the confined system, they are driven away from the hard obstacles or toward the centre of the micro-objects with restricted geometry. Of course, just the opposite behaviour has been observed for the molecules interacting through purely repulsive interaction potential.[83] Clearly, strongly repulsive molecules try to avoid each other such that they prefer the regions adjacent to the walls of the confinement. Such molecules are therefore accumulated next to the walls

to a greater extent than those incorporating some attractive interactions thus giving rise to more pronounced packing effects leading to more distinct layering structure and higher wall-fluid contact density of the fluid with repulsive particles. In the case of the model fluid of our present interest, which incorporates both repulsive and attractive interactions in the oscillating potential function one meets with a combination of all these effects. The resulting density profiles of confined fluid thus show the shapes arising from the complex interplay among the steric effects and the alternating repulsive and attractive parts of the effective potential. One can observe more or less sharp peak evolving at the distance $z = 1.5\sigma$ from the walls. This peak corresponds to the configuration of two successive molecular layers—the first comprising the molecules accumulated adjacent to the walls, and the second with the molecules strongly attached by the first layer. At bigger distances one sees the layering structure, the actual shape of the density profiles being governed by alternating repulsive and attractive intermolecular potential. This structure is not typical as found for the fluids with the molecules interacting via monotonically changing attractive or repulsive (tail) potential.[82,83] In the present case, successive molecules may feel qualitatively different (repulsive or attractive) interaction with their surrounding molecules. For this reason, as stated above in the discussion of the bulk structures, the density profiles show somewhat peculiar shapes also at bigger distances from the walls. A careful inspection of the results for the local structures of the fluid in different inhomogeneous systems indicates fair to very good agreement between the DFT predictions and simulation data.

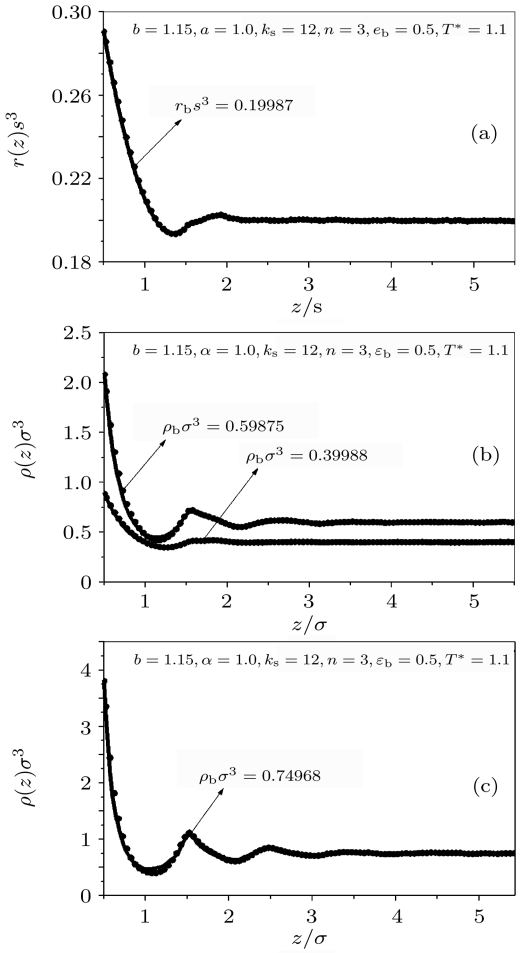



**Fig. 2.** The DFT (lines) and simulation (symbols) results for the density profiles of the fluid with the potential parameters $b = 1.15, \alpha = 1.0, k_s = 12, n = 3, \varepsilon_b = 0.5$ near a single hard wall at the reduced temperature $T^* = 1.1$ and at different values of the bulk density.

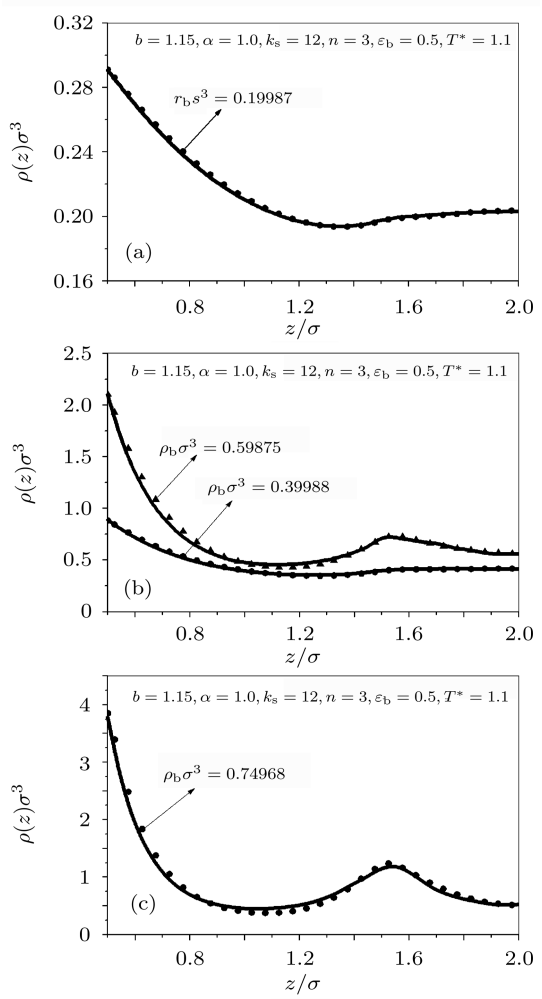



**Fig. 3.** The same as in Fig. 2 but in a planar gap of width $L = 4\sigma$.

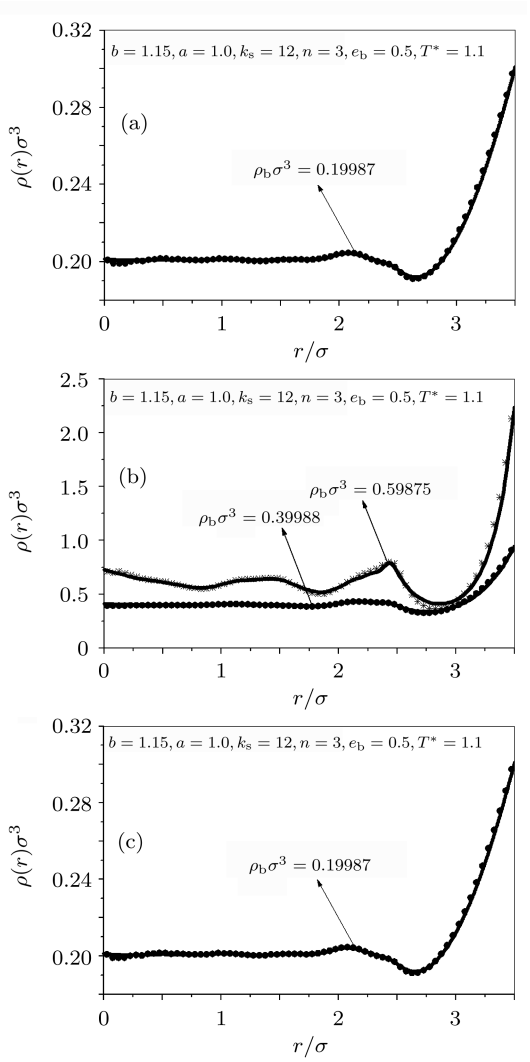



**Fig. 4.** The same as in Fig. 2 but in a spherical cavity of radius $R = 4\sigma$.

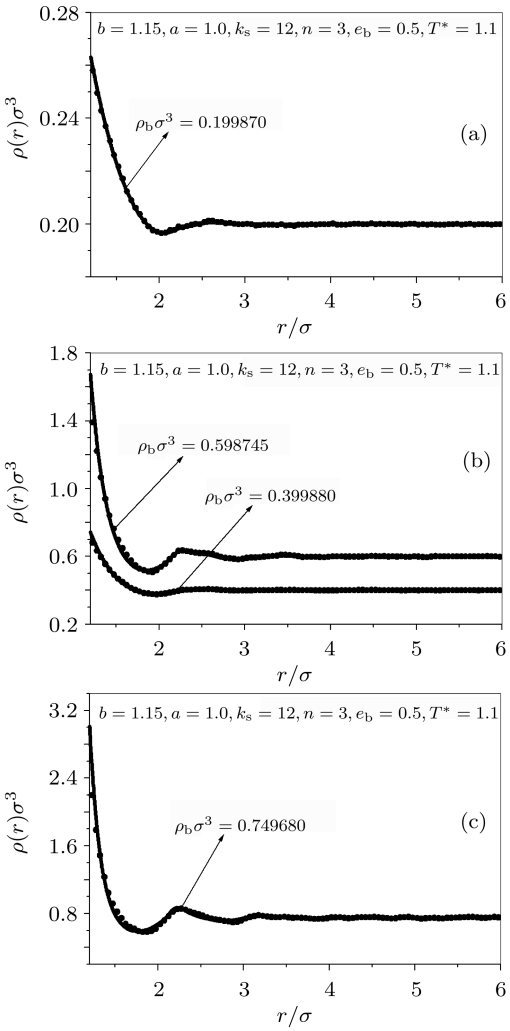



**Fig. 5.** The same as in Fig. 2 but near a hard spherical particle of radius $R = 0.7\sigma$.

# 4. Conclusion

The conclusion emerging from this work is that well-established approximate theories applicable for simple atomic fluids perform well also for the system of particles interacting through the effective potentials which are useful for the modeling of complex fluids. Recalling that validity of both the bridge function approximation and third order +second order perturbation DFT hinges on existence of a highly steep repulsive core, both the usual LJ potential and the presently chosen model effective potential are characterised with a hard sphere repulsion core, this supplies the possibility of the validity of the two tested theories exhibited for the chosen effective potential model. But coming true of such possibility truly mirrors the fact that tail contribution of the potential function does not play important role in the formation of structures. This is truly a structural counterpart of the van der Waals notion. The present investigation also indicates that the van der Waals notion also applies for inhomogeneous situation.

For those effective potential models which are not featured with the highly repulsive core, it is still an unsolved topic whether both the presently employed bridge function approximation and third order +second order perturbation DFT are also operative, more studies are needed. We will report relevant studies in the near future.

# References


[1] Patchkovskii S and Heine T 2009 *Phys. Rev.* E **80** 031603
[2] Sartarelli S A, Szybisz L and Urrutia I 2009 *Phys. Rev.* E **79** 011603
[3] Julin J, Napari I, Merikanto J and Vehkamäki H 2008 *J. Chem. Phys.* **129** 234506
[4] Lutsko J F 2008 *J. Chem. Phys.* **129** 244501
[5] Sun Z H and Han R J 2008 *Chin. Phys.* B **17** 3185
[6] Zhou S Q 2009 *J. Chem. Phys.* **131** 134702
[7] Bryk P and MacDowell L G 2008 *J. Chem. Phys.* **129** 104901
[8] Iwamatsu M 2008 *J. Chem. Phys.* **129** 104508
[9] Johannessen E, Gross J and Bedeaux D 2008 *J. Chem. Phys.* **129** 184703
[10] Zhang Y, Zhang Y and Zeng Y P 2008 *Chin. Phys.* B **17** 4645
[11] Zhou S Q 2004 *Chem. Phys. Lett.* **385** 208
[12] Zhou S Q 2003 *Phys. Lett.* A **319** 279
[13] Zhou S Q 2003 *Chin. Phys. Lett.* **20** 2107
[14] Ebner C, Saam W F and Stroud D 1976 *Phys. Rev.* A **14** 226
[15] Evans R 1979 *Adv. Phys.* **28** 143
[16] Nordholm S, Johnson M and Freasier B C 1980 *Aust. J. Chem.* **33** 2139
[17] Johnson M and Nordholm S 1981 *J. Chem. Phys.* **75** 1953
[18] Tarazona P 1985 *Phys. Rev.* A **31** 2672
[19] Curtin W A and Ashcroft N W 1985 *Phys. Rev.* A **32** 2909
[20] Rosenfeld Y 1989 *Phys. Rev. Lett.* **63** 980
[21] Kierlik E and Rosinberg M L 1990 *Phys. Rev.* A **42** 3382
[22] Capitán J A and Cuesta J A 2007 *Phys. Rev.* E **76** 011403
[23] Martínez-Ratón Y, Capitán J A and Cuesta J A 2008 *Phys. Rev.* E **77** 051205
[24] Zhou S Q and Ruckenstein E 2000 *Phys. Rev.* E **61** 2704
[25] Zhou S Q 2002 *New J. Phys.* **4** 36
[26] Zhou S Q 2002 *Chin. Phys. Lett.* **19** 1322
[27] Zhou S Q 2003 *Chem. Phys.* **289** 309
[28] Zhou S Q 2004 *J. Phys. Chem.* B **108** 3017
[29] Zhou S Q 2004 *Chem. Phys.* **297** 171
[30] Zhou S Q and Ruckenstein E 2000 *J. Chem. Phys.* **112** 8079
[31] Zhou S Q and Ruckenstein E 2000 *J. Chem. Phys.* **112** 5242
[32] Zhou S Q 2000 *J. Chem. Phys.* **113** 8719
[33] Zhou S Q 2001 *Phys. Rev.* E **63** 051203
[34] Zhou S Q 2001 *Phys. Rev.* E **63** 061206
[35] Zhou S Q 2001 *J. Phys. Chem.* B **105** 10360
[36] Zhou S Q 2008 *Chin. Phys.* B **17** 3812
[37] Zhou S Q 2001 *J. Chem. Phys.* **115** 2212
[38] Zhou S Q 2002 *Commun. Theor. Phys.* **37** 543
[39] Tang Z, Scriven L E and Davis H T 1991 *J. Chem. Phys.* **95** 2659
[40] Kol A and Laird B B 1997 *Mol. Phys.* **90** 951
[41] Sweatman M B 2001 *Phys. Rev.* E **63** 031102
[42] Kim S C and Lee S H 2004 *J. Phys.*: *Condens. Matter* **16** 6365
[43] Zhou S Q 2006 *Phys. Rev.* E **74** 031119
[44] Zhou S Q 2008 *Phys. Rev.* E **77** 041110
[45] Zhou S Q 2003 *Phys. Rev.* E **68** 061201
[46] Zhou S Q 2003 *Commun. Theor. Phys.* **40** 721
[47] Zhou S Q 2006 *J. Chem. Phys.* **124** 44501
[48] Zhou S Q 2005 *Int. J. Mod. Phys.* B **19** 4701
[49] Zhou S Q 2005 *J. Colloid Interface Sci.* **290** 364
[50] Zhou S Q 2006 *Int. J. Mod. Phys.* B **20** 469
[51] Zhou S Q 2006 *Mol. Simulat* **32** 1165
[52] Zhou S Q 2007 *Chin. Phys.* **16** 1167
[53] Zhou S Q 2010 *J. Chem. Phys.* **132** 194112
[54] Oxtoby D W 1990 *Nature* **347** 725
[55] Tang Z, Scriven L E and Davis H T 1992 *J. Chem. Phys.* **97** 494
[56] Patra C N and Ghosh S K 1993 *Phys. Rev.* E **48** 1154
[57] Tellez G and Trizac E 2003 *Phys. Rev.* E **68** 061401
[58] Patel N and Egorov S A 2004 *J. Chem. Phys.* **121** 4987
[59] Zhou S Q 2004 *Chem. Phys. Lett.* **392** 110
[60] Zhou S Q 2004 *Chem. Phys. Lett.* **399** 323
[61] Zhou S Q 2004 *Chem. Phys. Lett.* **399** 315
[62] Zhou S Q 2006 *Phys. Rev.* E **74** 011402
[63] Zhou S Q 2005 *J. Colloid and Interface Sci.* **288** 308
[64] Zhou S Q 2005 *Commun. Theor. Phys.* **43** 735
[65] Yan J Y 2008 *Chin. Phys.* B **17** 4640
[66] Chandler D, McCoy J D and Singer S J 1986 *J. Chem. Phys.* **85** 5971
[67] Yethiraj A 1998 *J. Chem. Phys.* **109** 3269
[68] van der Schoot P 2000 *Macromolecules* **33** 8497
[69] Zhou S Q and Zhang X 2001 *Phys. Rev.* E **64** 011112
[70] Zhou S Q 2005 *Chem. Phys.* **310** 129
[71] Zhou S Q 2006 *J. Colloid and Interface Sci.* **298** 31
[72] Asakura S and Oosawa F 1954 *J. Chem. Phys.* **22** 1255
[73] Vrij A 1976 *Pure Appl. Chem.* **48** 471
[74] Wax J F, Albaki R and Bretonnet J L 2000 *Phys. Rev.* B **62** 14818
[75] Moriarty J A and Widom M 1997 *Phys. Rev.* B **56** 7905
[76] Zhou S Q and Solana J R 2008 *Phys. Rev.* E **78** 021503
[77] Zhou S Q 2006 *J. Chem. Phys.* **125** 144518
[78] Zhou S Q 2007 *J. Phys. Chem.* B **111** 10736
[79] Zhou S Q 2008 *J. Chem. Phys.* **128** 104511
[80] Zhou S Q 2009 *J. Chem. Phys.* **130** 014502
[81] Zhou S Q and Solana J R 2009 *Chem. Rev.* **109** 2829
[82] Zhou S Q and Jamnik A 2006 *J. Phys. Chem.* B **110** 6924
[83] Zhou S Q 2006 *Commun. Theor. Phys.* (Beijing, China). **46** 323
[84] Henderson D 1992 *Fundamentals of Inhomogeneous Fluids* (New York: Marcel Dekker)
[85] Martynov G A 1992 *Fundamental Theory of Liquids. Method of Distribution Functions* (Bristol: Adam Hilger)
[86] Zhou S Q 2007 *Theor. Chem. Acc.* **117** 555
[87] Rosenfeld Y and Ashcroft N W 1979 *Phys. Rev.* A **20** 1208
[88] Frenkel D and Smit B 2001 *Understanding Molecular Simulation* (Boston, MA: Academic Press)
[89] Malasics A, Gillespie D and Boda D 2008 *J. Chem. Phys.* **128** 124102